International Journal of Mechanical Engineering and Applications
2022; 10(4): 82-89
http://www.sciencepublishinggroup.com/j/ijmea
doi: 10.11648/j.ijmea.20221004.15
ISSN: 2330-023X (Print); ISSN: 2330-0248 (Online)

Electrochemistry and Engineering Study of Molecular Protective-Films to Steel-Alloys

Desmond Teck Ching Ang[1, *], Peter Junk[2], Glen Deacon[3], Maria Forsyth[4]

[1]On-Time Engineering Consultancy Company, Singapore

[2]College of Sci & Engrg, James Cooks University, Townville, Australia

[3]School of Chemistry, Monash University, Clayton, Australia

[4]Institute for Frontier Materials, Deakin University, Burwood East, Australia

Email address:

angtc2013@gmail.com (Desmond Teck Ching Ang), angtc2008@yahoo.com.au (Desmond Teck Ching Ang)

[*]Corresponding author

To cite this article:

Desmond Teck Ching Ang, Peter Junk, Glen Deacon, Maria Forsyth. Electrochemistry and Engineering Study of Molecular Protective-Films to Steel-Alloys. *International Journal of Mechanical Engineering and Applications*. Vol. 10, No. 4, 2022, pp. 82-89.
doi: 10.11648/j.ijmea.20221004.15

Received: August 4, 2022; **Accepted**: August 23, 2022; **Published**: August 31, 2022

Abstract: The syntheses and characterisations of Rare-Earth-Metals (REMs) complexes, via the use of green organic esters such as Pyridinecarboxylate (Pyc) and hydroxylnaphthoate (Hnp) to form stable compounds ie. Lanthanide-hydroxylnaphthoate (Ln-Hnp), have been demonstrated to be the most preferred compounds to form a good protective-film over steel-alloys. The electrochemical techniques of Linear Polarisation Resistance (LPR) and Cyclic-Potentiodynamic Polarisation (CPP) used in the studies demonstrated strong protective properties to the steel-alloys from the *E* corr-potential and *I* corr-current. This is because the *I* corr-current was reduced by many folds when coupons were immersed in NaCl (0.01M) as a control bulk-electrolyte. The data has also confirmed that the Ln-Hnp complexes clearly displayed a mixed-type of protective function. Thus, the overall metal dissolution rate of steel alloys is mitigated and the data also indicated that it has shown a healing mechanistic process building a dense molecular composite-films up to 5-micron thick when alloy-coupons were immersed into the solution containing REMs complexes. The characterisation of in-situ treated surfaces by the use of ATR-FTIR microscopy and Raman spectrum revealed its overall protective characteristics which were discussed in this paper.

Keywords: Corrosion, Rare Earth Metals, Ligands, Coordination Chemistry, Electrochemistry

1. Introduction

Redox reactions of metal-alloys with its environments is a natural dynamic-processes. [1-9] This work is about REMs-complexes produced as green REMs-compounds, and for the purpose of studying the ability to protect steel-alloys. The characterisation of REMs-complexes and crystallography structures have been carried out. In summary, the formation of general composite protective-film is expressed as:

$$[Ln^{III}(L)_n]_{aq.} + y(OH^-) + x(Fe^{II}/Fe^{III})_{aq} + x(L^-)_{aq.} + H_2O \rightarrow [(Fe^{II/III})_x(Ln^{III})_n](L)_{n+x-y}(OH)_y + Ln(OH)_{3\ (ppt.)} \quad (1)$$

Electrochemistry defines redox reactions involving the loss of electrons during the metal dissolution and is termed as the anodic reaction as in Eq. 2. The partnering reduction reactions are named as cathodic reactions, as in equations 3 and 4, for examples:

$$Metal_{(solid)} \rightarrow M^{n+}{}_{(electrolyte\ IONS)} + ne^-{}_{(M\text{-}electrons)} \quad (2)$$

$$2H^+ + 2e^- \rightarrow H_{2(gas)} \quad (3)$$

$$O_2 + H_2O + 4e^- \rightarrow 4\ OH^- \quad (4)$$

The alteration of the electrochemical kinetics (rate) of metal dissolution via the modification of environments has become one of the fundamental methods in combating metal dissolution as corrosion. In 1970, organic inhibitors were described by G. Trabanelli and co-workers in “Mechanism and Phenomenology of Organic-inhibitors”. There was much preliminary work by

researchers at industries and universities. [10-14]. The research of organic compounds has become an important factor to induce a synergistic impact through formation of a reliable chemical binding, forming of high-density polymeric-sheet-style (coverage), which shall be resistant against the immediate environments. The present study of REM-organic complexes enhances the total synergistic impact, due to formation of lanthanide hydroxides $Ln(OH)_3$ in aqueous environments, which has an inherently low solubility in aqueous, over a wide range of pH between 5.5 to 13 and temperature conditions [15].

1.1. Materials and Preparations

1.1.1. Preparation of Lanthanide Ligand Complexes

A metathesis for synthesis and characterisation of complexes would be described as follow:

REM-organic complexes were produced at 90 +/-5°C within green aqueous media, $EtOH/H_2O$. Followed by evaporation for isolation of a single crystal.

Reagents and chemicals:

Ln_2O_3 (99.99%) and organic acid (99%) obtained from Sigma-Aldrich. Alkaline hydroxide (0.5M) solutions were prepared from sodium hydroxide or potassium hydroxide pellets and HCl, HNO_3 and H_2SO_4 were of AR grade. NaCl, Na_2H_2-EDTA laboratory grade reagent, used as received without further purification.

Lanthanide trivalent ion (Ln^{III}) solutions prepared from lanthanide oxides. Concentrations of lanthanide trivalent ion solutions are accurately determined by analysis using the titration with standardised 0.0100 M Na_2H_2-EDTA. Deionised water is always used in all preparation.

1.1.2. Preparation of Ligands' Salts

The Na(L) or K(L) prepared by reaction of Ligand (L-H) solution with NaOH or KOH (0.25 M) solution by monitoring the changes of pH to 8.5.

$$\text{Ligand-H} + \text{MOH} \rightarrow \text{M(L)} + H_2O \text{ (where M = K or Na)}$$

A general formula of lanthanide-organic complexes is expressed as

$$[Ln(L)_x(H_2O)_y.\ mH_2O]$$

Where:

Ln = REMs or Mm (Mischmetal ie. mixture of rare-earth elements).

L = Picolinate (Pic); isonicotinate (Isn) and 3-Hydroxy-2-naphthoate (3-Hnp).

1.2. Preparation of Protective REMs-Ligand Solutions and Complexes

1.2.1. REMs-Ligands Saturated Test Solutions

To D.I. water (pH range of 5.6-5.9), slowly stir an adequate amount of lanthanide-ligand complex while maintained temperature at 45 +/- 5°C for 3 hr. Removal of undissolved particles after solution is cooled to room temperature, add in NaCl 0.01M (10 mM) to inhibitor solutions for testing.

1.2.2. 3-Hnp-H Molecular Structure

Example of 3-Hnp-H molecular structure as presented in two orientations as shown in (a) & (b) diagrams.

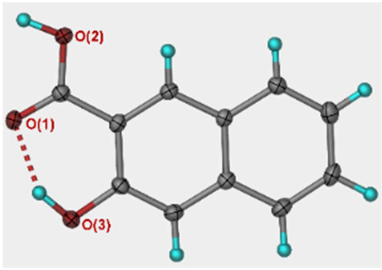

(a)

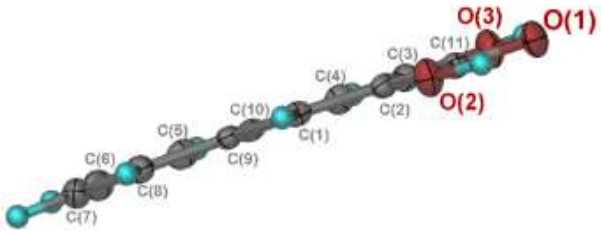

(b)

Figure 1. *3-Hnp-H molecular structure as presented in two orientations as shown in (a) & (b) diagrams.*

A yellow crystal prepared has a flat packing of 3-Hnp-H. The π-π interactions to the adjacent molecules are dominant features of the crystal packing diagram with C---C distances of 3.68 Å which compare well with examples reported in the Cambridge Crystallographic (CCDC) database. Intra-Molecular H-bonding bridges oxygen atoms of the hydroxyl and carboxyl groups in the solid state structure. The adjacent molecules are orientated in an opposite direction with respect to the salicylato functional group in the 3-Hnp core structure.

1.2.3. X-Ray Crystal Structure of REMs-Ligand Complexes

$[Ln(3\text{-Hnp})_3 \cdot m(H_2O)]_\infty$ complexes: [Ln = La, Ce and Pr]

The metathesis of sodium 3-Hnp with hydrated LnX_3 salts (X = Cl or NO_3) in water at pH 5.0 resulted in the precipitation of complexes, which were off-white for lanthanum, yellow for cerium and pale green for praseodymium. A general formula of these complexes is presented as $[Ln(3\text{-Hnp})_3].\ mH_2O$ [Ln = La, Ce and Pr]; m = 2 for La and m = 1.5 for Ce and Pr complexes. The aqueous synthesis afforded pure complexes in good yields: (La 82%, Ce 85% and Pr 86% respectively).

Example, $[Ce(3\text{-Hnp})_3(3\text{Hnp-H})]_\infty$: The X-ray crystal structure of $[Ce(3\text{-Hnp})_3(3\text{Hnp-H})]_\infty$ obtained good single crystal of complex mounts under a N_2 (-150°C) cold stream for X-ray diffraction analysis (see Figure 2).

The result of an eight coordinating $[Ce(3\text{-Hnp})_3(3\text{Hnp-H})]_\infty$ crystallised in the monoclinic ($P2_1/n$) space group. The cerium center is made up of $\mu\text{-}\eta^1{:}\eta^1$ bridging from six ligands, the Ce-O bond-lengths are 2.464(7), 2.420(7), 2.397(7), 2.448(7), 2.460(7), 2.440(8) Å. A protonated 3-

Hnp-H molecule forms a chelate via the oxygen atoms of a salicylato-group (*ortho*-hydroxyl and carboxylic acid); Ce-OOC, 2.556(8) Å and Ce-OH, 2.648(7) Å. It is noted that the bridging Ce-O distances are shorter by a value of 0.251Å when compared with the neutral ligand-chelating pair. This could be attributed to non-ionisation of the neutral ligand.

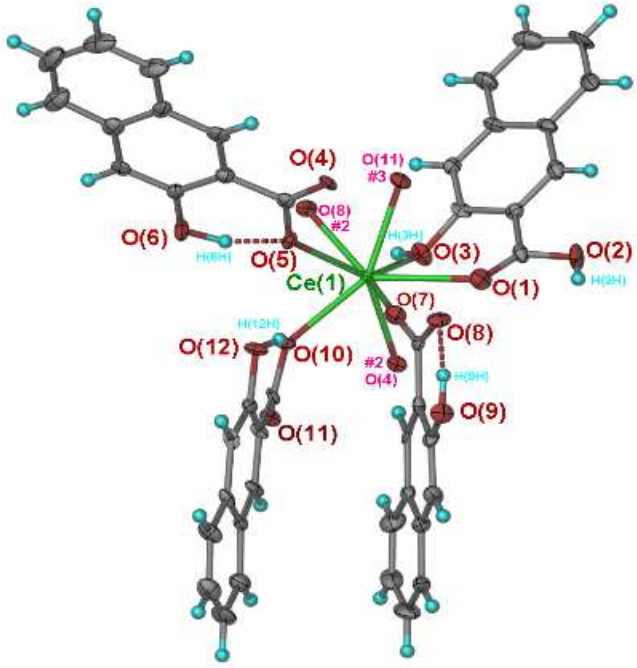

Figure 2. *[Ce(3-Hnp)$_3$(3Hnp-H)] was a yellow single crystal structure.*

1.2.4. Preparation of Steel-Alloy Coupons

Specimens are prepared from steel-alloy sheet: nominal composition are C, 0.04%; Mn, 0.24%; P, 0.007%; S, 0.009% and Fe, balance%. (Australia).

a) Immersion test samples cut size: 25 x 25 x 1 mm for ASTM G31-72.
b) Surface analytical samples size: 10 x 10 x 1 mm for ATR-FTIR, Raman spectroscopy and FTIR-imaging.
c) Electrochemical studies coupons size: 20 x 20 x 1 mm for ASTM G59-91 (LPR); ASTM G61-86 (CPP).

2. Results and Discussion of Studies

2.1. Overviews of Protective-Films Properties

To capture kinetic information, electrochemistry is commonly used as a preferred approach to bring an understanding of metal dissolving mechanistic rate.

2.2. Protective-Films and In-situ Surface Characterisation

Lanthanide (REMs) Organic complexes syntheses via a green pathway, for prelim screening to identify the preferred potential protective inhibitors. (1) Immersion test (ASTM G31-72, [16]) and (2) LPR as method (ASTM G59-91, [17]).

Immersion test of mass-loss results of ASTM G31-72 summarised in Table 1 and electrochemical data of ASTM G59-91 were recorded in Table 2, which is the measurement of *LPR (Rp)* Ohm.

Determination of steel alloy dissolution rate determined at aqueous environments, in the presence of REMs-complexes in bulk NaCl 100 mM (0.1 M) solution for immersion studies and at 10 mM (0.01 M) for electrochemical measurements of *LPR (Rp)* respectively.

Table 1. *Lab-Immersion test results (ASTM G31-72), after seven days within the solutions of different complexes; the reduction of steel-alloy dissolution rate compared to rate of control @ NaCl 0.10 M (100 mM) solution.*

(Ln$^{(III)}$ organic complexes) NaCl 0.10 M (100 mM)	Dissolution rate (7d) (µg / m^2-s) 33.6 (+/10%)	Comparison of protective efficacy (%) ***
3-Hnp-Ln (Ln=La; Ce; Pr; Mm (mixed REMs)	6.6; 4.5; 4.9; 4.3	81; 87; 85; 87
1-Hnp (1-hydroxy-2-naphthoate) Ce	8.9	73
Isn (isonicotinate) Ln (Ln =La; Ce; Pr)	15; 18; 18	46; 55; 56
Pic (picolinate) Ln (Ln =La; Ce; Pr)	27; 15; 18	19 / 46 / 45

*** Protective efficacy% = [(rate$_{(control)}$ – rate$_{(sample)}$) / rate$_{(control)}$] x 100%.

(a) Blank (b) one day (c) seven day

Figure 3. *A series of time-dependent studies w.r.t the bulk-solution containing [Ce(3-Hnp) (0.14 mM) @ NaCl 0.10 M (100 mM)].*

The efficacy study of Ce(3-Hnp)$_3$ complex on its protective strength is relatively effective, even after 50% (v/v) dilution with respect to saturated-solution of 100 ppm (0.14 mM) as 100%.

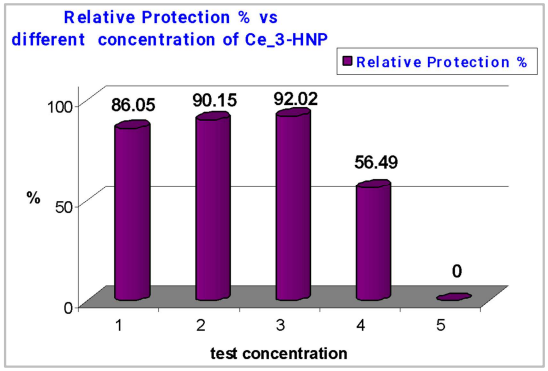

Denoted: 1 = 100% (saturated 0.14 mM Ce(3-Hnp)$_3$); 2 = 75% dil.; 3 = 50% dilution; 4 = 25% dilution; 5 = no inhibitor.

Figure 4. *ASTM G31-72 immersion tests showing the effectiveness of complex concentration for AS-steel coupon @ NaCl 0.10 M solution. (Tests were done between 33°C summer & 15°C winter seasons).*

2.2.1. Electrochemical Applications of LPR and CPP

(i). Linear-Polarisation Resistance (LPR) (ASTM G59-91) [18]

Table 2. *ASTM G59-91 Linear Polarisation Resistance (LPR) R_p(ohm) measured and tabulated.*

Inhibitors (Ln^{III} complexes)	***Rp* (K ohm) / E_{oc}(V)$_{(SCE)}$**	**Protective Efficacy% (***)**
NaCl (10mM)	1.9 / - 0.55 V	0
Isn-Ln	4.8 / -0.39V	60.4
La (200 ppm/ 0.41 mM)	5.5 / -0.37V	56.4
Ce (200 ppm/ 0.40 mM)	5.5 / -0.38V	56.4
Gd (200 ppm/ 0.39 mM)	3.2 / -0.31V	40.6
3-Hnp-Ln		
La (100 ppm/ 0.14 mM)	24.8 / -0.45V	92.3
Ce (100 ppm/ 0.14 mM)	25.3 / -0.38V	92.5
Pr (100 ppm/ 0.14 mM)	47.3 / -0.39V	96.0
Mm (100 ppm/ 0.14 mM)	28.5 / -0.38V	93.3

(***) Protection Efficacy = $[(R_{p\ (sample)} - R_{p(control)}) / R_{p(sample)}]$ x 100%.

Review (1): The results from both immersion-tests and *LPR* electrochemical data indicated lanthanide 3-hydroxy-2-naphthoate (3-Hnp) complex perform well in terms of the protective efficiency. This is showing 3-Hnp-H is stable poly-aromatic-hydrocarbon (PAH) compound, which consists of salicylato functional group i.e. carboxylate and ortho hydroxyl locate at 2, 3 position of core structure naphthalene 3-Hydroxy-2-naphthoic acid (3-Hnp-H).

(ii). CPP Data Analysis of Additives Containing Ce(Isn) and Ln 3-hydroxy 2-naphthoate (3-Hnp)

Table 3. *CPP Electrochemical data of Ce(Isn) series and Ln 3-hydroxy 2-naphthoate (3-Hnp) series extracted after the CPP scanning tests. @NaCl 10 mM (0.01 M) (All tests were conducted with conformance to ASTM G3-89 procedure).*

Complexes	**conc mM**	**E_{oc} V (-ve)**	**E_{corr} V (-ve)**	**log i_{corr} (mA/cm^2)**	**i_{corr} µA/cm^2**
NaCl control	10.00	-0.65	-0.59	-2.13	7.410
Ce(Isn)-1	0.92	-0.54	-0.58	-4.25	0.056
Ce(Isn)-2	1.84	-0.51	-0.51	-4.08	0.083
$CeCl_3$ hydrated	0.40	-0.68	- 0.67	- 3.52	0.302
Na(3-Hnp) salts	2.30	-0.58	- 0.58	- 3.20	0.631
Ce^{3+} +Na(3-Hnp)	(0.40 +2.3)	-0.58	- 0.59	- 4.50	0.032
Ce(3-Hnp) (STD)	0.14	-0.58	-0.50	- 5.10	0.010
Ce(3-Hnp) (AIR)	0.14	-0.51	-0.56	- 5.16	0.007
Mm(3Hnp) (STD)	0.14	-0.38	-0.39	- 4.33	0.047
Mm(3-Hnp) (AIR)	0.14	-0.50	-0.53	- 5.60	0.003
La(3-Hnp) (STD)	0.18	-0.35	-0.38	- 4.88	0.013
Pr(3-Hnp) (STD)	0.15	-0.41	-0.40	- 5.23	0.006

Where:
E_{oc} = open circuit after 24 h to achieve equilibrium state
E_{corr} = CPP forward scan corrosion potential
I_{corr} = CPP forward scan current density (mA / cm$^{2)}$ at E_{corr}.

The CPP scan-plots of Ce (Isn) solution at two different concentrations (Figure 5) indicated that both the anodic and cathodic current density arms are suppressed. Thus, it appears that this complex is truly mixed-type of protective function and has mitigated the dissolution-rate of iron alloy.

Investigation data shows clearly evidence of the synergy of the Ce(3-Hnp) complex by comparing to either each of individual compounds at comparable concentrations; *CPP* data reaffirmed Ln (3-Hnp) are behaving as mixed-type protector for steel-alloy with anodic behavior was dominating in the protection of iron surfaces as shown by Figure 6, Figure 7, Figure 8 and Figure 9.

The comparing i_{corr} of *CPP* plots for different Ln complexes, where Ln = La, Ce, Mm (mixed Ln). In which, it might suggest the combination of -OH and -COO groups at close proximity, allowing stronger coordination to the surface of laying metal substrate. There are researchers suggested that a bimetallic compound was forming with the Ce, Fe and the organic moiety.

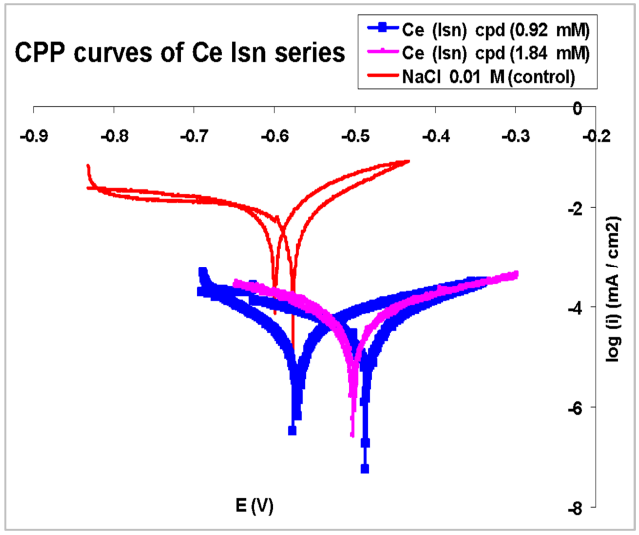

Figure 5. *CPP scan-plots of Ce (Isn) complexes Ce (Isn) (0.92 mM) in blue, Ce (Isn) (1.84 mM) in pink @NaCl (0.01 M) Control solution (zero inhibitor) in red.*

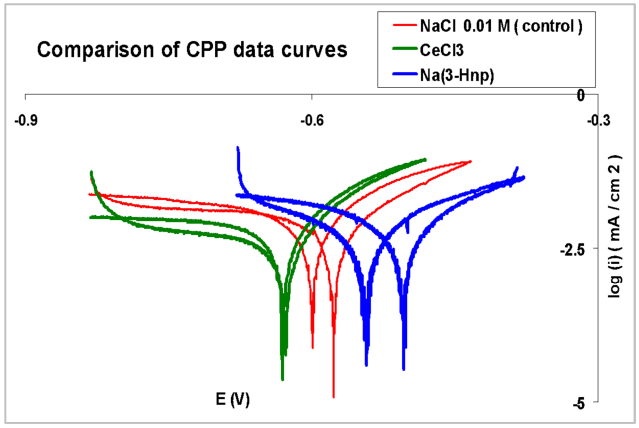

Figure 6. *Ln (3-Hnp) complexes CPP scan-cycle-plots $CeCl_3$ (0.40 mM) in green, Na(3-Hnp) 2.30 mM in blue and NaCl (0.01M) Control solution (zero inhibitor) in red.*

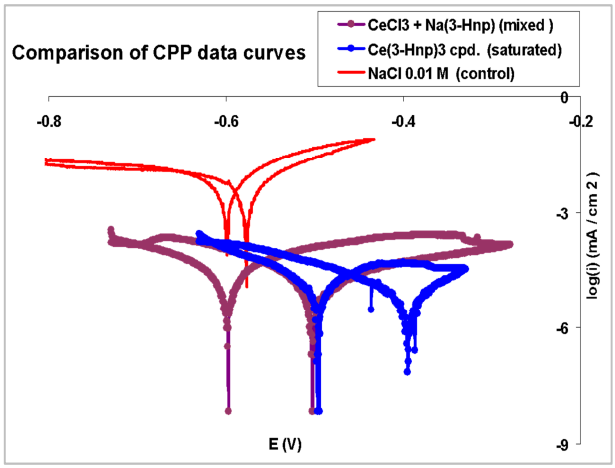

Figure 7. *CPP scan-cycle-plot of raw materials vs Ce 3-Hnp compounds i.e. Mixed of $CeCl_3$ + Na(3-Hnp) in purple vs Ce (3Hnp) complex (0.14 mM) in blue @NaCl 0.01 M control solution (zero inhibitor) in red.*

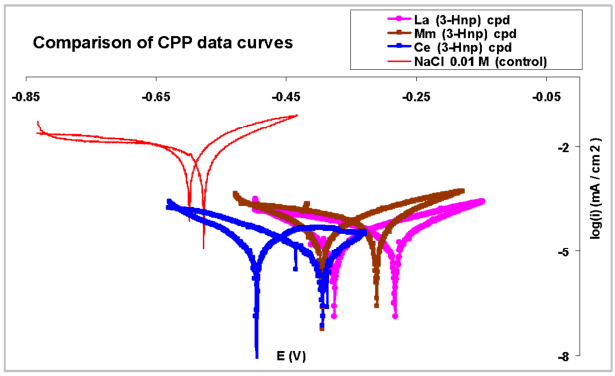

Figure 8. *CPP scan data of La, Ce and Misch metals (3-Hnp) complexes La (0.18 mM) in pink, Ce (0.14 mM) in blue, Mm (0.14 mM) in brown @ NaCl 0.01 M control solution (zero inhibitor) in red.*

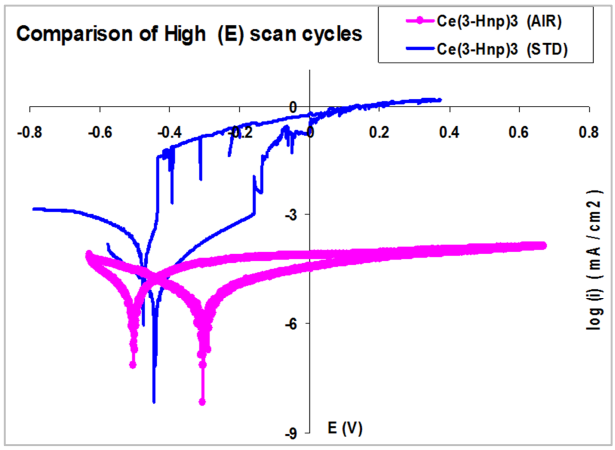

Figure 9. *CCP data curves of High E scan cycles for Ce(3-Hnp) (0.14 mM) (STD) in blue vs (AIR) in pink @ NaCl (0.01 M) as supportive electrolyte.*

Review (2): Comparison of CPP data between Ce(Isn) and Ln 3-hydroxy 2-naphthoate (3-Hnp).

Analysis of Electrochemical CPP data on E_{corr}, E_{rp} and i_{corr} has given a promising indication that protective-film is formed in the presence of REMs complexes. Lanthanide 3-hydroxy-2naphthoate (3-Hnp) that displayed as the

synergistic mixed-type anionic and cathodic protective inhibitor, at a relatively low concentration. Ln (3-Hnp) complexes are able to reduce the corrosion current density i_{corr} by three orders of magnitudes when compared to NaCl 0.01 M used as bulk-supportive electrolyte.

The Ln (3-Hnp) complex interestingly illustrated is a strong and stable protective-film under the aeration (O_2 rich) condition, which is exhibiting symptoms of auto-healing effects that may be possible within the reality of environments.

2.2.2. In-situ Surface Characterisation by Spectroscopy [19-23]

To survey the mechanistic and characteristics of in-situ corroding metal-surfaces conditions by using electrochemical techniques, jointly with the modern electromagnetic radiation technologies; to get an insight of corroding mechanistic on metal dissolution at the molecular level. Therefore, *in-situ* techniques with the use of microscopic imaging technologies provide an overall view of the scientific path to understand the detrimental processes of the metals corrosion issue.

ATR-FTIR spectroscopy technique is commonly used in studying the interfacial chemistry of surface structures of water-goethite (-FeO·OH). In which, the binding modes of salicylato organic compounds to iron oxides reported by Humbert and co-workers. They applied Infrared and Raman spectroscopic technique to investigate the interaction of iron with organic salicylato anion.

(i). Lanthanide Isonicotinate Ln(Isn) ATR-FTIR

Table 4. *ATR FTIR spectra bands of Fe (Isn) and Ce (Isn) compounds with assignments.*

	Metal-oxygen zone ע				COO (sym) ע
Ce(Isn) (complex)	680	766	1006	1152	1395
Fe(Isn) (crystal)	618	743	1018	1145	1375
Fe(Isn) (coupon)	619	742	1019	1161	1377

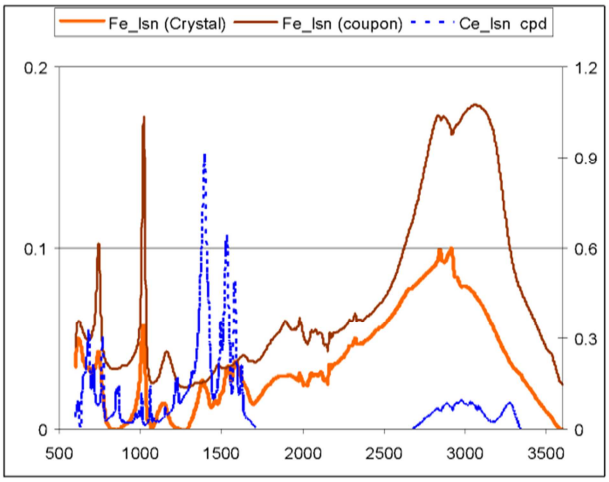

Figure 10. *ATR-FTIR spectra of Fe (Isn) and Ce (Isn) review spectra on Finger-print regions (500 to 1800 cm^{-1}).*

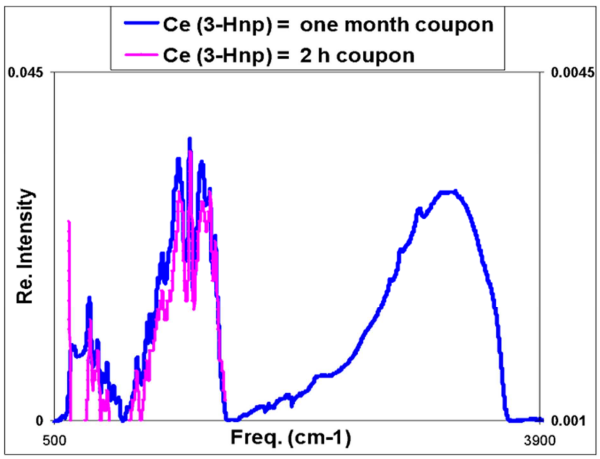

Figure 11. *ATR-FTIR spectra of coupons treated with Ce(3-Hnp) for one month and 2 h tests @ NaCl 0.01M.*

In comparison to the ATR-FTIR spectra Table 4, the shifted bands of Ce^{III} (Isn) and Fe^{II} (Isn) between metal-ligand binding regions (500 to 1000 cm^{-1}). The strong possibility of bimetallic compounds co-existed on the steel surface to be certified.

Interestingly noted that FTIR spectra have shown strongly suggested that a reliable passive-film was stable throughout the entire study period of one-month immersion. It is once again suggested that the formation of low solubility metallic (3-Hnp) compound appeared to be a good stable film, which is resistant in aqueous solution containing chloride anions.

(iii). Raman Spectroscopy In-situ Surface and Characterization of Ce 3-Hnp and AS-steel Alloy Coupons

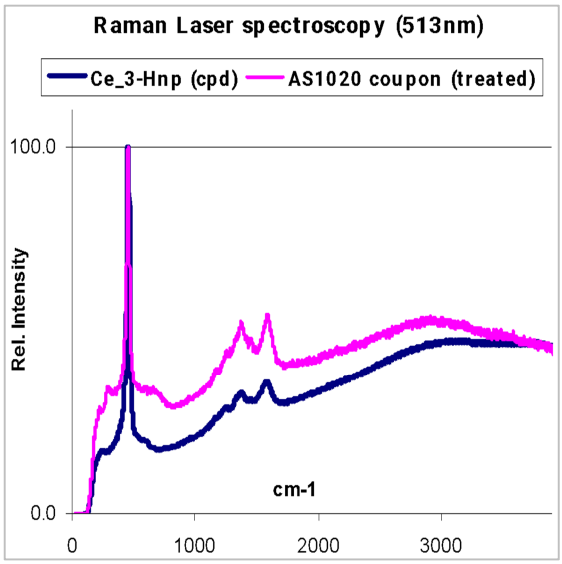

Figure 12. *Raman laser spectroscopy (513 nm) in-situ surface analysis of steel-alloy coupon by @ after Ce(3-Hnp) treatment.*

Table 5. *Raman spectroscopy (513 nm) spectrum assignments to in-situ surface analysis of steel-alloy coupon by @ after Ce(3-Hnp) treatment.*

Ce(3-Hnp)	AS-steel alloy coupon
455 (s)	453 (s)
1243 (m)	1232 (m)
1368 (s)	1359 (s)
1405 (m)	1417 (m)
1576 (s)	1561 (s)
2883 (m, br)	2961 (m, br)

Raman spectroscopic results on a treated steel-iron alloy coupon in a solution of Ce(3-Hnp) were captured with the use of a filtered laser beam of 513 nm (green colour) in the studies. The advanced optical layout of the Renishaw-micro system used a narrow sample window (1µm) which is to provide strong signals for Raman shift analyses. From the in-situ surface analysis of spectra data captured by using Raman 513 nm to scan on steel-iron coupon, after being treated within a bulk solution of NaCl 0.01 M containing Ce(3-Hnp) complex. The Raman shifts clearly displayed that the treated coupons were covered with the presence of Ce(3-Hnp) as protective-films. The spectrum indicated the formation of the passive film on steel-coupons, after they were immersed in a NaCl solution (0.01M) containing Ce(3-Hnp) (0.14 mM). These results again support the previous data obtained from electrochemical experiments.

(iv). EDAX Surface Analysis of In-situ Steel-Alloy Coupons

Steel-alloy coupons were subject for EDAX analysis after treatment with a NaCl (0.01 M) solution containing Ce(3-Hnp) (0.14 mM). The coupons surface covered with a dark-brown product. EDAX investigation found cerium and iron co-existed within the dark passive-film. Qualitative analysis data showed cerium was present on the coupons at a low ratio to iron (see Figure 13). A SEM photo image of the coupon (see Figure 14) showing a rough topographic view of deposits is fully covered on the surface of steel-alloy coupons at the accumulated thickness of 5.359 µm.

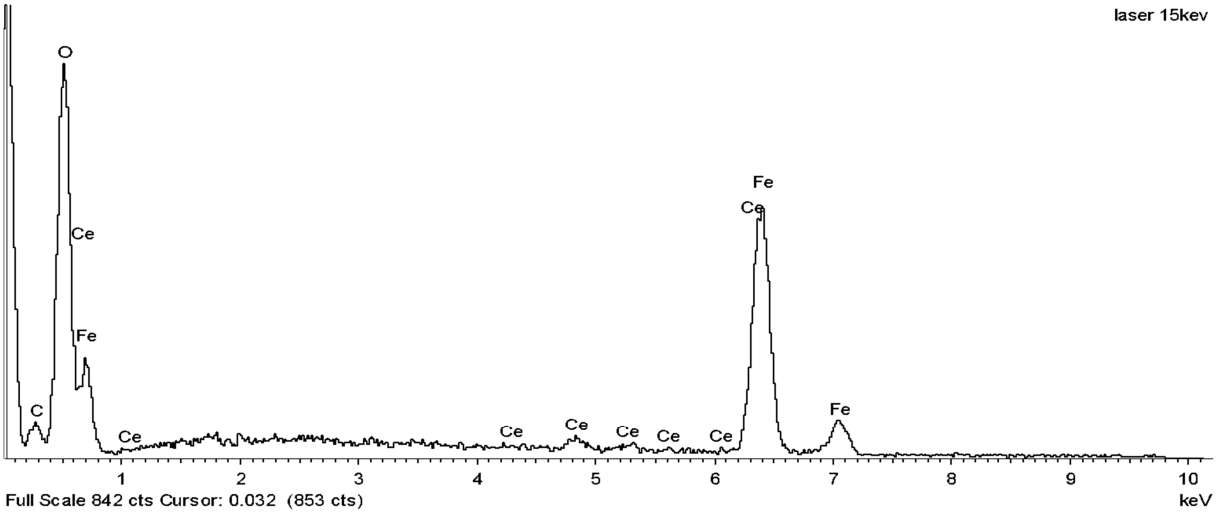

EDAX Spectrum [relatively intensity]

Figure 13. *EDAX elemental spectrum of steel-allyo coupon surface after one-month of treatment with NaCl 0.01 M solution containing Ce(3-Hnp)$_3$ (0.14 mM).*

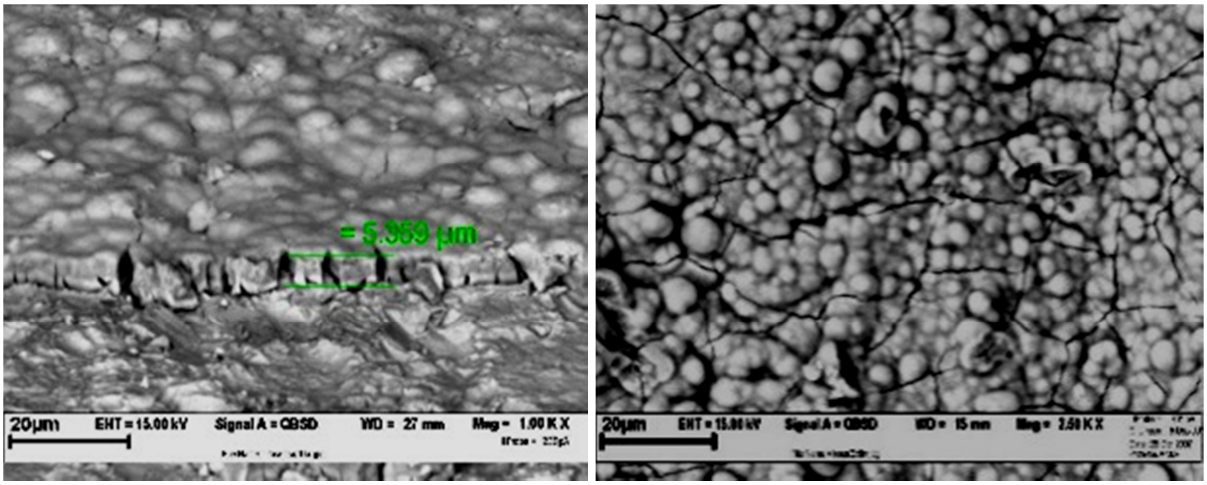

(a) Thickness of passive film = 5.359 µm (b) Topography of passive film and crack-line under SEM vacuum

Figure 14. *(a) and (b): SEM photo images of steel coupon surface after one-month treatment with NaCl 0.01 M solution containing Ce(3-Hnp)$_3$ (0.14 mM).*

Review (3) of in-situ surface characterisation of Ln(3-Hnp) compound with the use of ATR-FTIR and Raman spectra confirmed a stable passive-film is present on the steel-alloy coupons, upon treatment in NaCl (0.01 M) bulk solution which is containing lanthanide pyridinecarboxlyate (Pyc) or hydroxlynaphthoate (Hnp) complexes. However, the mechanistic of corrosion mitigation process and the composition of the passive-film require further investigation. The synergistic effect of the protective layer formed by Ln (3-Hnp) towards iron steel-alloy surfaces.

Corrosion processes is a series of hetero-chemical-reaction that are much environmentally dependence. Therefore, to combat corrosion by mitigating metal-dissolution is required to deal with, by the combination of science and engineering technologies [24-26].

3. Conclusion

The prelim results are derived from the immersion-tests and *LPR/CPP* electrochemical data are presented in Table 1 and 2. We are confident that lanthanide 3-hydroxy-2-naphthaote (3-Hnp) performs well in terms of the protective efficacy for steel-alloy. The Ln (3-Hnp) complex has interestingly illustrated that it has a strong stability protective-film under tests with an aeration of oxygen rich condition, and exhibiting a potential auto-healing effect which occurs in real-life application conditions.

Acknowledgements

The author greatly appreciates Prof. Peter Junk, Prof. Glen Deacon and Prof. Maria Forsyth for their guidance and assistance rendered during the entire work of my study. Added greatest appreciation to Mr. Alvin Y. W. Ang who has been given unconditional support in preparation of the paper.

References

[1] J. O. M. Bockris, S. U. M. Khan, Surface ElectroChemistry (A molecular Level approach), Plenum Press, New York & London, 1993.

[2] D. Tytgat, B. Solvay et Cie., (Ed.: E. P. Appl.) p. 21 French, 1981.

[3] V. R. Pludex, "Design and Corrosion Control", John Wiley and Sons, USA, 1997.

[4] F. Blin, (PhD Thesis), Monash University (Melbourne, Australia.), 2005.

[5] N. Hackerman, E. S. J. Snavely, J. S. J. Payne, Journal of The Electrochemical Society, 113, no 7, 677, USA 1966.

[6] H. J. Leidheiser, I. Suzuki, J. Electrochem. Soc. p 128, 242, 1981.

[7] A. Kula, Journal of Thermal Analysis and Calorimetry, 68, 957. 2002.

[8] G. Trabanelli, V. Carrassiti, in Advanced in Corrosion Science and Technology, Vol. vol 1 (Eds.: M. G. Fontana, R. W. Staehle), Plenum Press, New York-London, p. 147, 1970.

[9] M. Stern, *Corrosion* 1958, *14*, 440.

[10] K. E. Wilson, (PhD Thesis), Monash University, Australia (Melbourne), 2004.

[11] T. Behrsing, (PhD Thesis) Monash University, Australia (Melbourne), 2003.

[12] R. G. Kelly, D. W. Shoessmith, R. G. Buchheit, *Electrochemical Techniques in corr. Sci & Engrg*, Marcel Dekker Inc, NY, 2003.

[13] B. R. W. Hinton, A. Raman, P. Labine, in *Corrosion / '89 paper no. I-11, p 1*, NACE, 1989.

[14] Yost-E., W. Zeltner, M. Machesky, M. I. Tejedor-Tejedor, M. Anderson, in *Geochemical Processes at Mineral Surfaces, Vol. 323, ACS*, ACS Symposium Series 323, Washington, DC., 1986, p. 142.

[15] C. H. Evans, Biochemistry of the Lanthanides, Plenum Press, New York & London, 1990.

[16] ASTM, in ASTM, G31-72 (Ed.: ASTM), p. 7, 1999.

[17] ASTM, in ASTM, G59-91 (Ed.: ASTM), p. 4, Philadelphia, USA, 1991.

[18] ASTM, in *ASTM G3-89* (Ed.: ASTM), ASTM, Philadelphia, USA, 1991, 1991, p. 8.

[19] M. Biber, W. Stumm, *Environ. Sci. Techno* 1994, *28*, 763.

[20] B. Humbert, M. Alnot, F. Quiles, *Spectrochimica Acta (Part A)* 1998, *54*, 465.

[21] M. C. Alverez-Ros, S. Sanchez-Cortes, J. V. Garcia-Ramos, *Spectrochim. Acta (Part A)* 2000, *56*, 2471.

[22] G. B. Deacon, C. M. Forsyth, T. Behrsing, K. Konstas, M. Forsyth, *Chem. Commun.* 2002, 2820.

[23] A. Paneque, J. Fernandez-Bertran, E. Reguera, H. Yee-Madeira, *Spectr. Lett.* 2003, *36 (1 & 2)*, 83.

[24] W. Lewandowiski, M. Kalinowska, H. Lewandowiska, *J. of Inorg. Biochem.* 2005, *99*, 1407.

[25] R. M. Cornell, U. Schwertmann, *The Iron Oxides*, VCH, 1996.

[26] F. A. Cotton, G. Wilkinson, *Advanced Inorganic Chemistry*, 4th ed., John Wiley & Sons, 1980.